Field monitoring and analysis of an onshore wind turbine shallow foundation system

Jesús González-Hurtado, Pengpeng He, Tim Newson & Hanping Hong
Geotechnical Research Centre, Department of Civil Engineering, Western University, London, Ontario, Canada.
Melanie Postman & Sheri Molnar
Department of Earth Sciences, Western University, London, Ontario, Canada.

ABSTRACT
Investigations of the soil-foundation interaction behaviour and transfer of energy from the wind to the ground and the subsequent transmission of elastic waves to the surrounding areas have not been conducted in Ontario. Indeed, very few seismic monitoring studies have been conducted globally around wind farms. It has been found that turbines predominantly produce vibrations related to structural resonances and blade passing frequencies. Spectral peaks correlated with wind speed, and spectral composition and energy was found to be modified with distance and was dominated by surface waves. This paper discusses a study of the effect of the wind-structure interaction on the behaviour of a turbine foundation and the generation of ground-based vibrations around a working commercial wind turbine. The field monitoring system and meteorological instrumentation are described in this paper and the responses of the structure and the surrounding ground due to the fluctuating wind-field are discussed.

RÉSUMÉ
Les enquêtes sur le comportement d'interaction sol-fondation et le transfert d'énergie du vent au sol et (à)la transmission subséquente d'ondes élastiques dans les zones environnantes n'ont pas été menées en Ontario. En effet, très peu d'études de surveillance sismique ont été menées autour des parcs éoliens(dans le monde entier) Il a été constaté que les turbines produisent principalement des vibrations liées aux résonances structurelles et aux fréquences de passage des lames. Les pics spectraux étaient en corrélation avec la vitesse du vent. (En outre)la composition spectrale et l'énergie se sont révélées (d')être modifiées avec la distance et étaient dominées par les ondes de surface. Cet article traite d'une étude de l'effet (d'interaction de vent structurel) sur le comportement d'une base de turbine et (de) la génération de vibrations au sol autour d'une éolienne commerciale (fonctionné). （De plus) Le système de surveillance sur le terrain et l'instrumentation météorologique sont décrits dans cet article et les réponses de la structure et du terrain environnant (causé par) terrain éolien fluctuant sont discutées.

1 INTRODUCTION

Wind is a major source of renewable energy and has been the largest source of new electricity in Canada for the last 11 years as reported by CANWEA (2017). By the end of 2016 there were 11,898 MW of total installed wind energy capacity in the whole country, enough to account for around 6% of its electricity demand. The province of Ontario has the largest wind market in Canada and is projected to capture 11% of the energy generation capacity for the province by 2018 (CANWEA, 2011).

Wind turbines are subjected to millions of load cycles throughout their entire service lives due to environmental and mechanical loads. Understanding the behavior of the wind turbine foundation in response to this complex cyclical vertical-horizontal-moment loading plays an important role in turbine design. Investigations of the soil-foundation interaction behaviour and transfer of energy from the wind through the tower to the ground and the subsequent transmission of elastic waves to the surrounding areas have not been conducted in Ontario. Indeed, very few seismic monitoring studies have been conducted globally around wind farms. Saccorotti et al. (2011) and Xi et al. (2014) found that turbines predominantly produce vibrations related to structural resonances and blade passing frequencies. Spectral peaks correlated with wind speed, and spectral composition and energy was significantly modified with distance and was dominated by surface waves. Further studies by Styles et al. (2005) and Fiori et al. (2009) found maximum RMS velocities on turbine foundations ranging between 0.07-0.15 mm/sec. Edwards (2015) found 125 m from a specific turbine that RMS velocities of 0.001 mm/sec occur.

In Ontario, a minimum offset distance of 550 m between residents and vibration sources, such as wind turbines, is mandatory. However, this distance seems to be related to acoustic criteria and is less than the majority of other jurisdictions in North America and Europe. Further work is needed to help establish the distance at which the elastic wavefield at the base of the wind turbine structures is no longer present (or sensible) with distance, to better understand the significance of setback distances.

A multi-disciplinary research project is underway to investigate the behavior of a commercial wind turbine founded on a shallow foundation and underlain by a carbonate-rich glacial clay till deposit in Southern Ontario. One goal of the project is to provide understanding of the effect of the wind-structure interaction on the behaviour of the turbine foundation and the generation of ground-based vibrations around the turbine. A detailed site investigation

has been conducted on the site and a full-scale monitoring system has been installed on the wind turbine. The field foundation monitoring system and meteorological instrumentation are described in this paper and the responses of the structure and the surrounding ground due to the fluctuating wind-field during the monitoring are discussed.

2 SITE CONDITIONS

The wind turbine in this study, is located in a relatively simple topographic and geological area in the Great Lakes region of Southern Ontario. The turbine is part of a commercial wind farm near Lake Erie, with a total of 88 turbines. This specific turbine model produces a nominal power of 2.3 MW, has a hub height of 80 m and triple blade rotor with a 93 m diameter. The wind turbine is supported by a shallow octagonal foundation, with approximate dimensions of 19 m in diameter and 3 m depth, and is underlain by a carbonate-rich glacial clay till deposit. A meteorological tower featuring 5 anemometers at different heights, is located 150 m North-West of the wind turbine.

2.1 Soil Profile from Field and Laboratory Data

To characterize the soil profile at the site, four boreholes were drilled adjacent to the turbine foundation to depths twice the foundation diameter. Soil samples were collected at 3 m depth intervals. *In-situ* testing was also performed, and consisted of standard penetration test (SPT), seismic cone penetration test (SCPTu), cross-hole seismic testing (CST) and field shear vane (FSV). To complement the *in-situ* testing, various laboratory tests were carried out as well. Among the laboratory tests are consolidated isotropic undrained triaxial tests (CIU test), oedometer tests, bender element tests (BE test) and resonant column tests (RCA test). For more detailed information on the testing results refer to previous papers and reports from the authors (Gonzalez-Hurtado and Newson, 2013 and 2016; Tyldesley et al., 2013; Kiss, 2016).

The study area was found to be underlain by a carbonate-rich glacial clay till deposit of approximately 40 to 45 m thickness. The deposit can be approximately split into three different layers. A heavily weathered oxidized upper crust between 0 and 1.5 m, a partially weathered lower crust that transitions from an oxidized to an unoxidized state, between 1.5 and 4.5 m and an un-weathered clay till from 4.5m to a depth that 40 m. Figures 1 and 2 show the strength and stiffness data derived from *in-situ* and laboratory tests. The marked difference between the layers is shown in both the undrained shear strength profile (S_u) and the small-strain shear modulus (G_o) profiles with depth. The wind turbine foundation sits approximately at the peak strength/stiffness zone of the soil profile (at 3 to 4 m depth). In addition to that, it can be seen how the values of strength and stiffness (S_u and G_o) reduce rapidly to relatively uniform values at depths of 6 to 8 m, maintaining this trend in the underlying 12 to 15 m. From Figures 1 and 2 it is also noticeable that there is relatively good agreement between the various characterization methods used to obtain the aforementioned properties of the soil profile on the site.

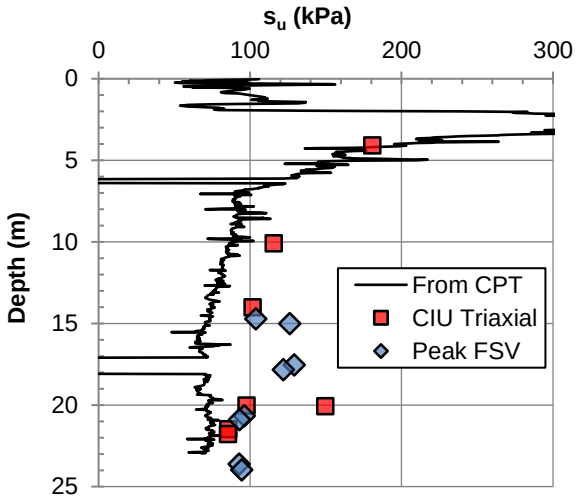

Figure 1. Undrained shear strength (s_u) with depth (after Tyldesley et al., 2013)

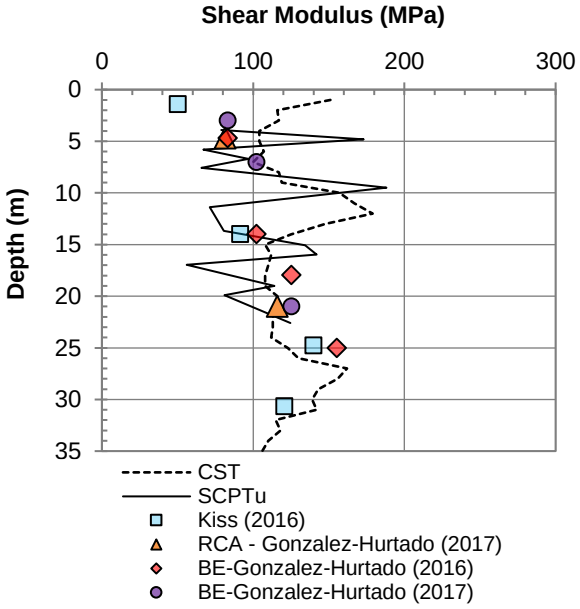

Figure 2. Small-strain shear modulus (G_o) with depth

2.2 IEC Classification and Design Wind Speeds

The wind farm has been classified as an IEC 61400-1 Class IIb site; this categorizes the area as having medium level turbulence intensity and wind speeds (IEC 61400-1). The expected value of the turbulence intensity at a wind speed of 15 m/s for a class IIb is 14% and the reference 50-year return period 10-minute average wind speed is specified as 42.5 m/s. The project site specific extreme value 50-year 10-minute average wind speeds have been estimated as 33.9 m/s. The annual average wind speed at hub height is 8.5 m/s and the 50-year return period 3 second gust wind speed is 59.5 m/s.

3 FIELD MONITORING SYSTEM

3.1 Foundation monitoring

The current foundation monitoring system includes four uniaxial tiltmeters and three portable high frequency triaxial seismometers, (known as Tromino®) and one triaxial accelerometer (see Figure 3). The sampling rates of the tiltmeter, Trominos and accelerometer are 20, 128 and 20 Hz, respectively. Results from the tiltmeters have been reported before by Kiss et al. (2014) and will not be repeated here. The Trominos can capture velocities in 3 directions simultaneously, with an accuracy of ±1.2 mm/s at full scale, that can be recorded in a frequency range between 0.1 Hz to 200 Hz. The tiltmeters (denoted as TM1, 2, 3 and 4) are placed at the four cardinal directions to measure the rotation of the foundation in the N-S and E-W directions. The triaxial accelerometer, located at N0, can measure accelerations between -3g to +3g with a bandwidth range of 0.5 Hz to 50 Hz. The accelerometer is installed at the same position as TM2 (see Figure 3), and the three Trominos are located at 30 (N1), 130 (N2) and 300 m (N3) to the North of the foundation edge, respectively. Vibrations towards the N and E cardinal directions have been taken as positive. In this paper, only data obtained from N0 to N3 are used to analyze the wave propagation induced by the vibration of the wind turbine foundation.

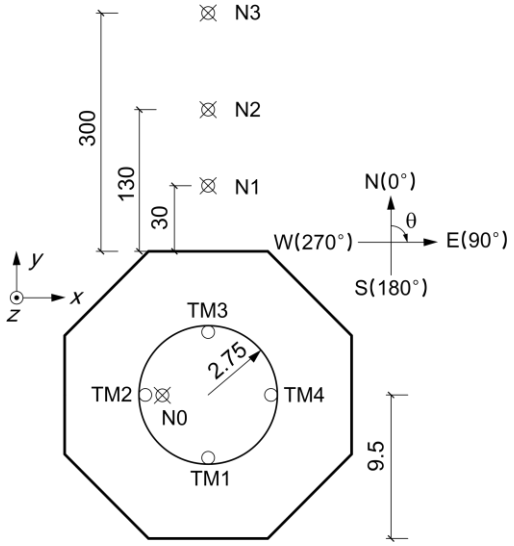

Figure 3. Diagram of foundation and location of the instrumentation (all dimensions in Meters) – not to scale.

3.2 Wind monitoring

Wind speed and direction variation over the study time period should be characterized to relate the response of the foundation to the incoming wind field. The speed and direction of the wind is measured from 5 cup anemometers located on a meteorological tower (MET) tower (at 34, 61, 70, 77 and 80 m above ground level) located 150 m to the North-West of the wind turbine and the turbine nacelle (80 m). The wind data is collected every 1 second. In this paper, only the wind data measured at the nacelle (80 m) is used.

4 RECORDED DATA

4.1 Typical Foundation Data and Analysis

Table 1 lists the recording periods of the triaxial accelerometer (N0) and the Trominos located at N1 to N3. The recording period of the wind was over two days, but only the period corresponding to that of the Trominos is extracted, as shown in Table 1.

Table 1. Adjusted start and end times of N1, N2, N3 and wind speed

Sensor Location	Date	Start Time	End Time	Time Recorded
N0 (0 m)	11-10-2016	09:49:10	11:08:24	1h 19' 14''
N1 (30 m)	11-10-2016	09:49:10	11:17:47	1h 28' 37''
N2 (130 m)	11-10-2016	09:49:10	11:29:57	1h 40' 47''
N3 (300 m)	11-10-2016	09:49:10	10:31:41	0h 42' 31''
Wind	11-10-2016	09:49:10	11:29:57	1h 40' 47''

The measured wind velocities and wind direction over the study period are shown in Figure 4. As can be seen from Figure 4a, the wind speed remains relatively stable except for a slight increase during the last 2000 seconds (around 30 mins). The mean value and the RMS (root-mean-square) level of the wind speed over this period is 9.85 m/s and 1.31 m/s. Following the definition of turbulence intensity outlined by Burton et al. (2001), the turbulence intensity of the measured wind is 0.13. As shown in Figure 4b, the wind direction (θ) during the recording period is primarily from the southwest direction (between 220 and 250 degrees – southwest to west-southwest). Overall, the wind speed and wind direction did not change significantly, allowing a reasonable characterization of the statistics of the behaviour of the wind and soil vibrations.

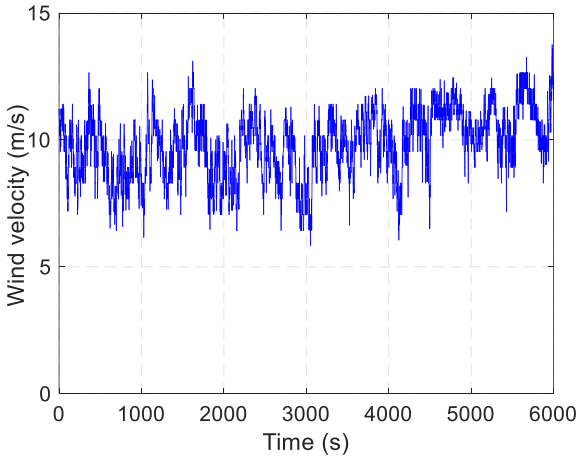

a)

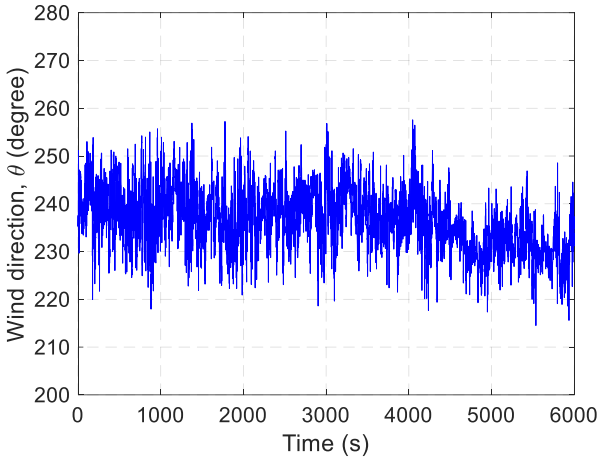

b)

Figure 4. Measured (a) wind velocity and (b) wind direction

Figure 5 illustrates the time-history of the acceleration in the positive *x* (eastern) direction at locations N0 to N3. It is obvious that the acceleration at N0 on the foundation is much higher than the acceleration at the other three locations due to the proximity of the vibration source. It can be seen from Figure 5(a) that the positive part of the acceleration is relatively higher and fluctuates more than the negative part of the acceleration. This may be attributed to two reasons: firstly, the turbine wake flow can induce a negative pressure at the back of the wind turbine, pulling the wind turbine in the positive *x* direction, the second is that the wind direction is in the southwest direction, which is not consistent with the positive *x* direction of the accelerometer at N0.

Comparison between the accelerations at N0 to N3 (Figure 5b, c and d) shows that the acceleration amplitude rapidly decreases with distance. The amplitude of the acceleration at N1 is about 0.8% of that at N0. The amplitudes at N1 and N2 are similar, but negligible compared with N0 and N1 due to energy dissipation caused by the underlying soil.

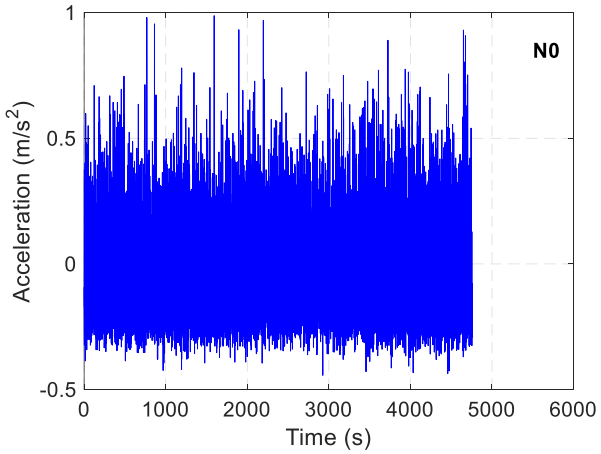

a)

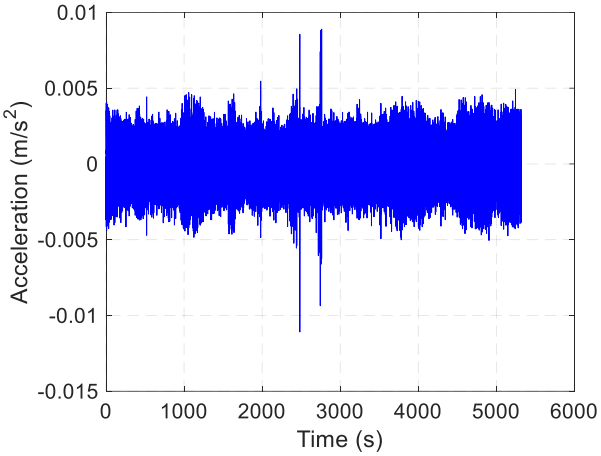

b)

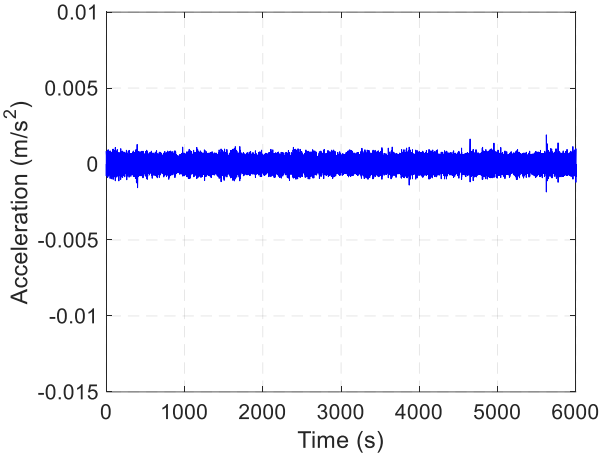

c)

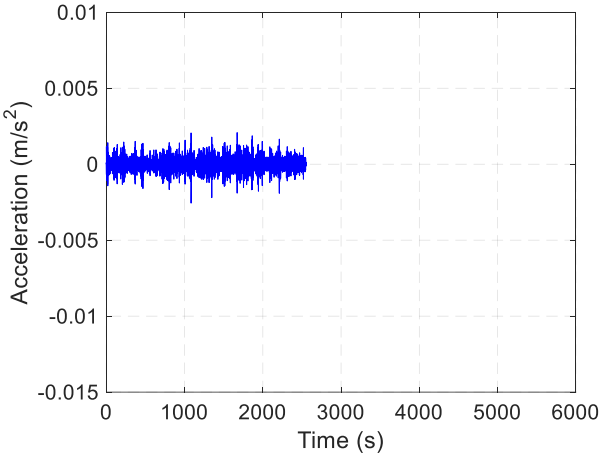

d)

Figure 5. Time-history acceleration in the *x* direction at locations (a) N0, (b) N1, (c) N2 and (d) N3

The power spectral density (PSD) of the acceleration in the *x* direction at N0 to N3 is shown in Figure 6. PSD is used to describe the spectral energy distribution with

frequencies so that the dominant frequency ranges can be specified. The sampling rates of the accelerometer and the Trominos are 20 and 128 Hz, respectively, so the maximum frequencies that can be captured are 10 and 64 Hz according to the Nyquist sampling criterion. As shown in Figure 6(a), the frequency measured at the N0 is widely distributed in the ranges from 0 to 8 Hz. The PSD of the acceleration at N0 peaks at around 0.2 to 0.5 Hz and gradually decreases to zero with frequency. Two peaks occur for the PSD of the acceleration at N1 and N2, around 9 and 25 Hz. A comparison between Figure 6(b) and 6(c) indicates that the dominant frequency at N1 is of a higher frequency band, while at N2 the lower frequency band is more predominant. This can be attributed to the fact that high frequency vibrations attenuate more rapidly than low frequency vibrations (Stoll & Bryan, 1970). Interestingly, the PSD at N3 has a peak corresponding to a higher frequency, ranging from 40 to 55 Hz, probably because of wave dispersion in the soil. Comparison between the amplitudes at these four locations confirms that the energy decreases as shown in Figure 5.

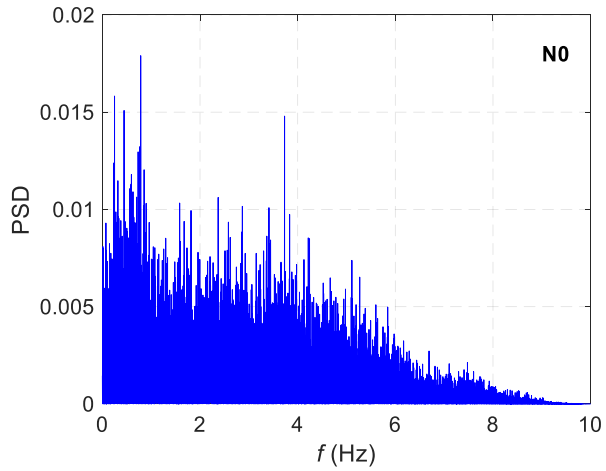

a)

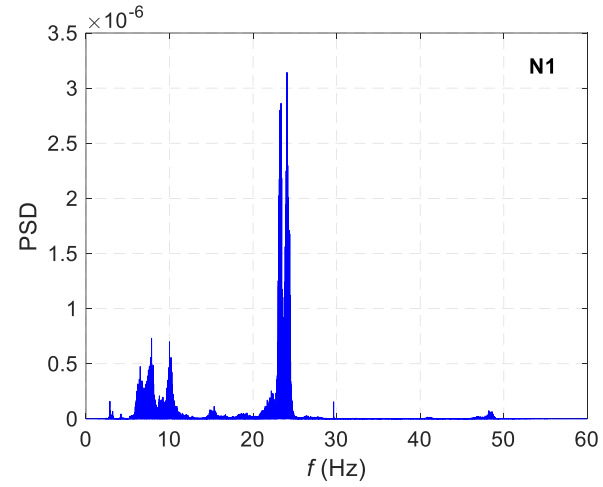

b)

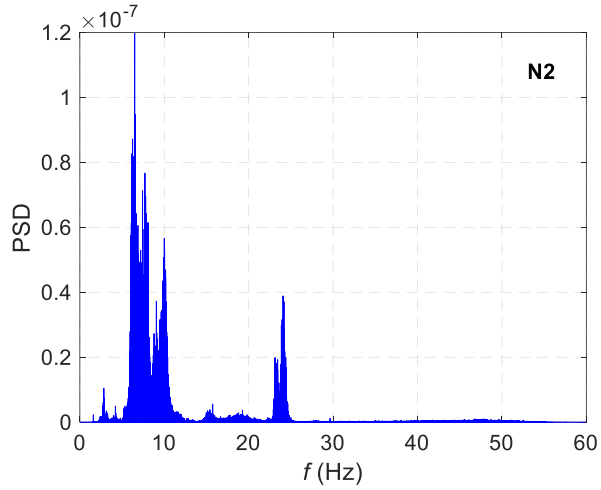

c)

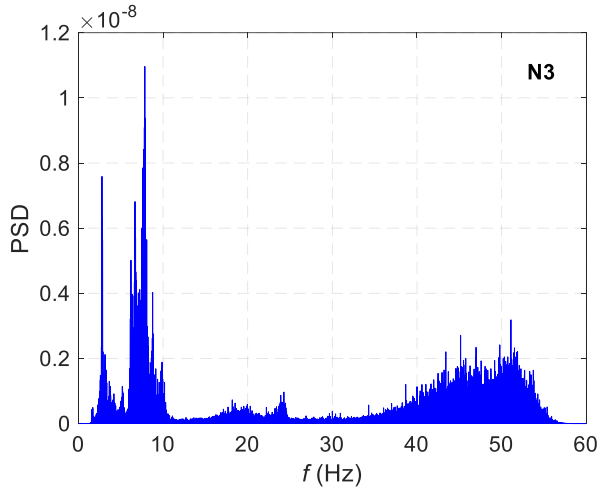

d)

Figure 6. PSD of the acceleration in the *x* direction at locations (a) N0, (b) N1, (c) N2 and (d) N3

Figure 7 shows the time-history of the acceleration in the *y* and *z* direction at location N1. Compared with the amplitude of the acceleration in the *x*-direction shown in Figure 5b, the amplitudes in the *y* and *z* direction are relatively smaller. It can be noticed that two peaks are observed in Figure 6b and Figure 7, and these two peaks in the *y* direction (Figure 7a) are higher than those in the *x* (Figure 5b) and *z* (Figure 7b) direction. This may be primarily due to across-wind vortex shedding from the turbine tower.

To assess the properties of the wave propagation in the soil, particle motions are compiled in Figure 8. As shown in Figure 8(a), the *x*-*z* (vertical-longitudinal) direction motions are approximately counter-clockwise ellipses. Vibration in the *y* (transverse) component is smaller compared with that in the *z* (vertical) direction as shown in Figure 8(b). The particle motions at N3 (Figure 8c) imply that the particle motions gradually become circles in the *x*-*z* direction with the increase of distance from the vibration source.

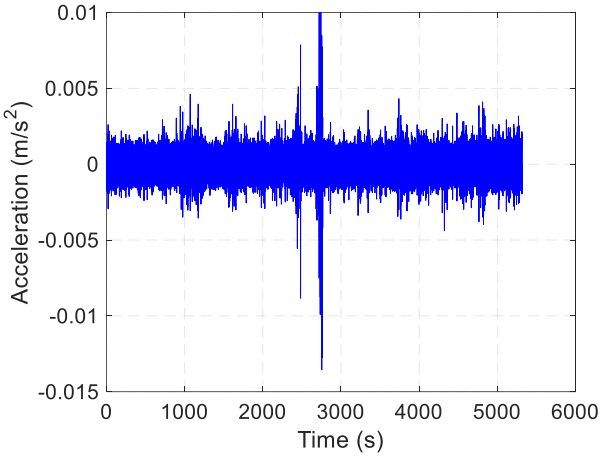

a)

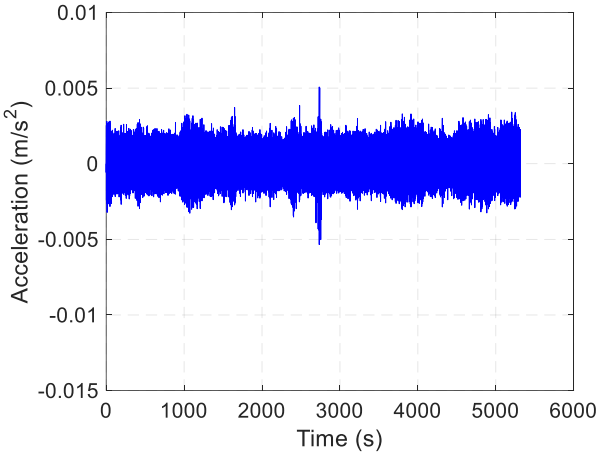

b)

Figure 7 Time-history of the acceleration in the *y* and *z* direction at location N1 (a) *y* direction and (b) *z* direction

Although these types of elliptical motions are usually associated with Rayleigh wave propagation (Kim & Lee, 2000), it should be noted that the axes of both sets of ellipses are apparently tilted in Figures 8 (a and b), towards the assumed direction of propagation. This may in part be due to the difference in the measurement and wind axes. However, Crampin (1975) and Tanimoto (2004) also noted that these types of tilted elliptical particle motions occur with surface waves propagating through anisotropic and layered media. In this form of material, the particle motions remain elliptical, but the plane of polarization deviates from the propagating direction by a certain angle, leading to a more complex 3D quasi-Rayleigh behaviour with additional transverse soil motions.

The energy contained by the propagating waves and their amplitudes, will decrease with increasing of the distance from the vibration source, where they were generated. Velocity attenuation in soil with distance on the ground surface is illustrated in Figure 9. The mean values and standard deviation of the velocities at locations N0 to N3 are calculated and represented by the error bars. Data measured at N0 to N3 is employed to demonstrate the velocity attenuation relationship with distance.

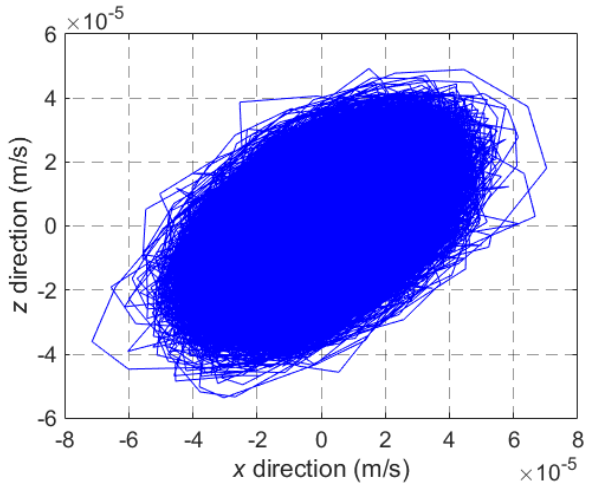

a)

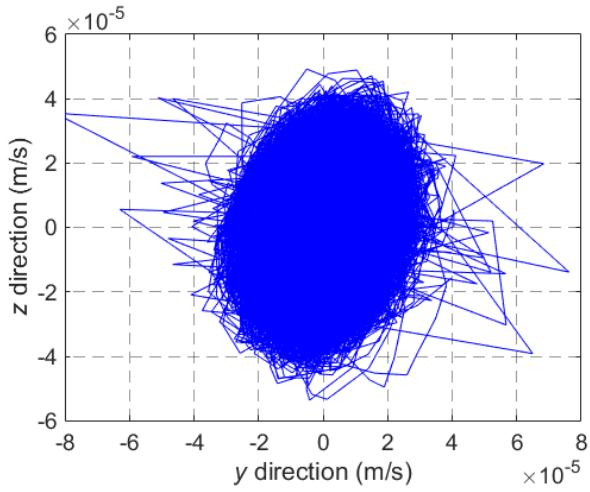

b)

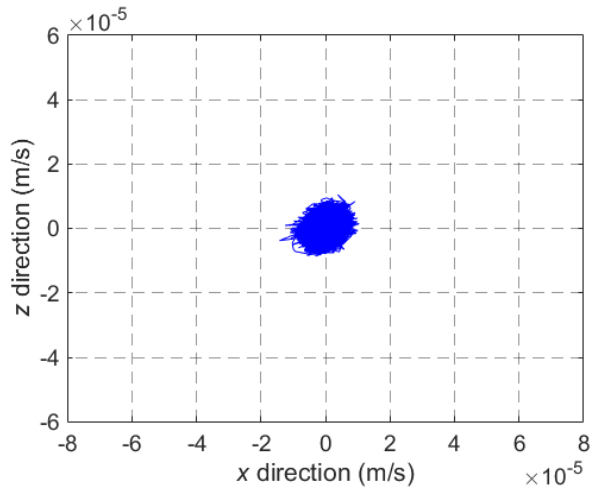

c)

Figure 8. Particle motions at N1: (a) *x*-*z* direction and (b) *y*-*z* direction; and at N3: (c) *x*-*z* direction

As shown in Figure 9, the attenuation in the *x* and *y* direction is similar except for a slight difference between the amplitudes of N1 and N2. This field data indicates vibration velocities comparable with those seen in previous studies, in the range of 0.04-0.07 mm/sec 30 m from the foundation to 0.001-0.003 mm/sec 300m from the foundation.

Energy dissipation can be attributed to soil damping, e.g. geometric damping (radiation) and material damping, and the attenuation relationship has been evaluated with the following equation (Kim & Lee, 2000):

$$w_2 = w_1 \left(\frac{r_1}{r_2} \right)^n e^{-\alpha(r_2 - r_1)} \quad [1]$$

where w_2 and w_1 are the amplitudes at distance r_2 and r_1 from the vibration source; n and α are geometric and material damping coefficients respectively. The material damping coefficient can be evaluated with:

$$\alpha = \frac{\pi \eta f}{c} \quad [2]$$

where η is a loss factor; f is the wave frequency; c is the wave propagation.

As described above, the propagating wave has been assumed to be primarily a Rayleigh wave, so Rayleigh wave velocity is used in Eq. 2. The average Rayleigh wave velocity of the ground soil is estimated to be 262.8 m/s from the cross-hole test. According to Figure 6, the dominant frequency of 8 Hz is selected. The value of η is given as 0.5 for clay by Gutowski and Dym (1976). Therefore, the material damping coefficient α can be calculated as 0.0478 for both *x* and *y* directions from Eq. 2.

To examine the effect of the geometric and material damping, two fitting curves are applied: the first one only considers the geometric attenuation by setting the material damping coefficient α to be 0 (shown by the red solid line in Figure 9); the other one takes both the geometric attenuation and the material attenuation into consideration by using α=0.0478 (see the black dashed line in Figure 9). As shown in Figure 9, the fitted geometric damping coefficients in the *x* and *y* directions are 1.41 and 0.71 respectively without considering material attenuation. Therefore, the rate of geometric attenuation in the *x* direction is relatively larger than that in the *y* direction. In contrast, the presence of material attenuation significantly increases the attenuation rate with distance. Comparison shows that primarily geometric attenuation can favorably describe the observed attenuation of the vibration amplitudes.

The value of the geometric coefficient (n) is related to the decrease of energy density with distance from the source. This is a function of the source type and the form of wave propagation. Gutowski and Dym (1976) reported values of n from different vibration field cases, e.g. traffic and train lines, pile driving, hydraulic compaction and blasting. These values ranged from zero to 2 depending on the nature of the waves (surface/body) and type of source (surface/buried and line/point). A point source producing purely Rayleigh waves in a homogeneous isotropic elastic half-space would have a value of n=1.5, which is relatively close to that found in the x direction.

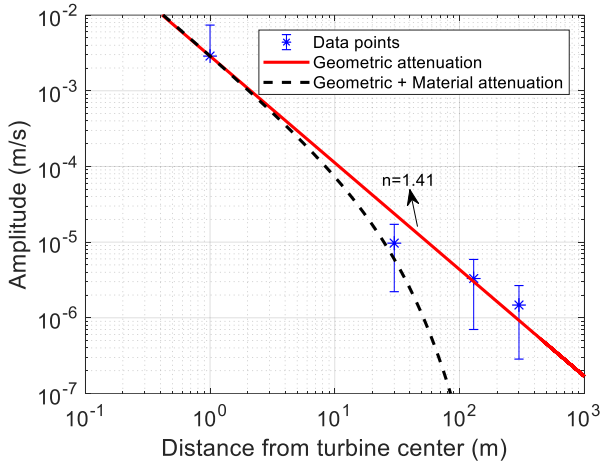

a)

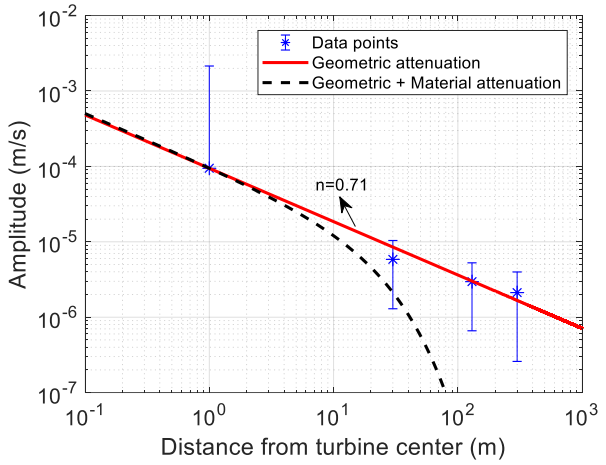

b)

Figure 9. Velocity attenuation with distance: (a) *x* direction; (b) *y* direction

5 SUMMARY & CONCLUSIONS

The dynamic response of a wind turbine, located in the Great Lakes region of Southern Ontario, has been investigated with field tests. The wind data, foundation vibration data and ground motion data were obtained. The vibrations in different directions at four locations have been analyzed and compared.

The vibration acceleration amplitudes in the *x* (longitudinal) and *z* (vertical) directions are relatively larger than those in the *y* (transverse) direction, since the wind direction is primarily from the west-southwest to southwest direction, which is relatively close to the *x* axis (see Figure 3). The comparison between the dominant frequency ranges at different locations shows that the higher frequency vibrations attenuate more rapidly than the lower frequency vibrations. The observed propagating elastic wavefront at some distance from the turbine appears to be

dominated by surface waves and shows some influence of the presence of anisotropy or layering in the soil profile.

The vibration of the foundation caused by the operation of wind turbines appears to rapidly decrease with distance from the vibration source. Generally, geometric and material attenuation should be both incorporated, but the analysis indicates that the geometric attenuation plays a more important role than the material attenuation for this site and material. The presence of material damping can decrease the vibration amplitudes more rapidly. The comparison between the two fitting curves in Figure 9 shows that the discrepancy increases with distance and the recorded data coincide with the geometric attenuation, which means that the effect of material damping is negligible in the far field for this site. From the analysis of Kim & Lee (2000), the combination of these two attenuation factors can favorably describe the amplitude attenuation relationship with distance in the near field (within 100 m). Therefore, the vibration attenuation may be dominated by both geometric and material attenuation in the near field, whilst only geometric attenuation occurs in the far field.

The 'subset' of the data presented in this paper is consistent with a full recorded dataset, which examined vibrations in two other directions (west and south) from the turbine. No dependence of recording location and wind direction was found (Postman, 2017). Further work is required to confirm these findings for a range of wind speeds and directions, and different locations around the site, as well as for different operating conditions of the turbine.

ACKNOWLEDGEMENTS

The writers would like to acknowledge the help and support of J.J Davis from Kruger Energy and the Western CES Seed Grant fund. The financial support of NSERC for the first and second author is acknowledged. The second author is also grateful for the financial support of China Scholarship Council (CSC).

REFERENCES

Burton, T., Sharpe, D., Jenkins, N., and Bossanyi, E. 2001. *Wind Energy Handbook*, John Wiley & Sons, Hoboken, NJ, USA.

Crampin, S. 1975. Distinctive Particle Motion of Surface Waves as a Diagnostic of Anisotropic Layering, *Geophysical Journal International*, 40(2): 177-186.

Edwards, W.N. 2015. *Analysis of Measured Wind Turbine Seismic Noise Generated from the Summerside Wind Farm, Prince Edward Island*, Geological Survey of Canada, Open File 7763.

Fiori, I., Giordano, L., Hild, S., Losurdo, G., Marchetti, E., Mayer, G. and Paoletti F. 2009. A study of the seismic disturbance produced by the wind park near the gravitational wave detector, *GEO-600 3rd International Meeting on Wind Turbine Noise*, Aalborg, Denmark.

Gonzalez-Hurtado, J. and Newson, T. 2014. Determination of rigidity index for a shallow foundation on a carbonate clay till, *Canadian Geotechnical Society: Geo Regina*, Regina, Canada. Paper # 227.

Gonzalez-Hurtado, J. and Newson, T. 2016. Small-strain behaviour of a carbonate clay till underlying a wind turbine shallow foundation by different in-situ and laboratory tests, *Canadian Geotechnical Society: Geo Vancouver*, Vancouver, Canada. Paper # 3653.

Gutowski, T.G. and Dym, C.L. 1976. Propagation of ground vibration: a review, *Journal of Sound and Vibration*, 49(2): 179-193.

Kim, D.S. and Lee, J.S. 2000. Propagation and attenuation characteristics of various ground vibrations, *Soil Dynamics and Earthquake Eng.* 19(2): 115-126.

Kiss, J. 2016. *Evaluation of the response of carbonate clay beneath a wind turbine foundation*. (MESc. Thesis). London, Ontario, Canada: Department of Civil and Environmental Engineering, Western University.

Kiss, J., Newson, T. and Miller, C. 2014. The effect of wind-structure interaction on the behavior of a shallow wind turbine foundation, *Canadian Geotechnical Society: Geo Regina*. Regina, Canada. Paper # 231.

Peterka, J. 1992. Improved extreme wind prediction for the United States, *Journal of Wind Engineering and Industrial Aerodynamics*, 41(1-3), 533-541.

Postman, M. 2017. *Vibration monitoring at a Wind turbine site in Port Alma, Ontario*. (BSc. Thesis). London, Ontario, Canada: Department of Earth Sciences (Geophysics), Western University.

Saccorotti, G., Piccinini, D., Cauchie, L. and Fiori, I. 2011. Seismic noise by wind farms: a case study from the Virgo Gravitational Wave Observatory, Italy, *Bulletin of the Seismological Society of America*, 101(2), 568-578.

Stoll, R.D. and Bryan, G.M. 1970. Wave attenuation in saturated sediments, *The Journal of the Acoustical Society of America.* 47(5B): 1440-1447.

Styles, P., Stimpson, I., Toon, S., England, R. and Wright, M. 2005. Microseismic and infrasound monitoring of low frequency noise and vibrations from windfarms: recommendations on the siting of windfarms in the vicinity of Eskdalemuir, Scotland, *Keele University (UK), Report for the Ministry of Defence*, 18.

Tanimoto, T. 2004. The azimuthal dependence of surface wave polarization in a slightly anisotropic medium, *Geophysical Journal International.* 156(1): 73-78.

Tyldesley, M., Newson, T., Boone, S. and Carriveau, R. 2013. Characterization of the geotechnical properties of a carbonate clayey silt till for a shallow wind turbine foundation, *18th International Conference on Soil Mechanics and Geotechnical Engineering.* CFMS, Paris, France, 1: 2407-2410.

Xi Engineering Consultants Ltd. 2014. *Seismic vibration produced by wind turbines in the Eskdalemuir region*. Release 2.0, Report No: FMB_203_FINAL_VSR.